Strong thermal fluctuations in cuprate superconductors in magnetic fields above T_c

Xujiang Jiang,[1,2] Dingping Li,[1,2,*] and Baruch Rosenstein[3,†]
[1]*School of Physics, Peking University, Beijing 100871, China.*
[2]*Collaborative Innovation Center of Quantum Matter, Beijing, China*
[3]*Electrophysics Department, National Chiao Tung University, Hsinchu 30050, Taiwan, Republic of China*
(Received 28 July 2013; revised manuscript received 4 February 2014; published 18 February 2014)

Recent measurements of fluctuation diamagnetism in high-temperature superconductors show distinct features above and below T_c, which can not be explained by simple Gaussian fluctuation theory. Self-consistent calculation of magnetization in layered high-temperature superconductors, based on the Ginzburg-Landau-Lawrence-Doniach model and including all Landau levels is presented. The results agree well with the experimental data in a wide region around T_c, including both the vortex liquid below T_c and the normal state above T_c. The Gaussian fluctuation theory significantly overestimates the diamagnetism for strong fluctuations. It is demonstrated that the intersection point of magnetization curves appears in the region where the lowest Landau level contribution dominates and magnetization just below T_c is nonmonotonic. Our calculation supports the phase disordering picture of fluctuations above T_c.

DOI: 10.1103/PhysRevB.89.064507 PACS number(s): 74.20.De, 74.25.Bt, 74.25.Ha, 74.40.−n

I. INTRODUCTION

One of the numerous qualitative differences between high-T_c superconductors (HTSCs) and low-T_c superconductors is dramatic enhancement of thermal fluctuation effects. The thermal fluctuations are much stronger in HTSC not just due to higher critical temperatures; much shorter coherence length and high anisotropy play a major role in the enhancement too. Since thermal fluctuations are strong the effect of superconducting correlations (pairing) can extend into the normal state well above the critical temperature especially in the presence of strong magnetic field that further enhances the fluctuations. The normal state properties of the underdoped cuprates exhibit a number of anomalies collectively referred to as the pseudogap physics [1] and their physical origin is still not clear despite a remarkable theoretical effort [2–5] to establish a microscopic theory. It is natural, therefore, to attempt to associate some of these phenomena with the superconducting thermal fluctuations or preformed Cooper pairs [6–8].

The interest in fluctuations was invigorated after the Nernst effect was observed [9–11] all the way up to the pseudogap crossover temperature T^* in underdoped $La_{2-x}Sr_xCuO_4$ (LSCO). Assuming that the Nernst effect is primarily due to thermal fluctuations, the whole pseudogap region would be associated with preformed Cooper pairs and become a precursor of the superconducting state. The finding motivated additional experiments on the Nernst effect in various HTSCs [12], as well as renewed study of thermal fluctuations in the temperature region between T_c and T^* by other probes: electric [13–15] and thermal conductivity [16] and diamagnetism [17]. The main goal was to try to quantify the superconducting fluctuation effects, so they can be either directly linked or separated from the pseudogap physics. This requires a reliable quantitative theory of influence of thermal fluctuations of superconducting order parameter on transport (Nernst effect, thermal, and electric conductivity) and thermodynamic (magnetization, specific heat) physical quantities. Since there is no sufficiently simple and/or widely accepted microscopic theory of HTSC, one has to rely on a more phenomenological Ginzburg-Landau (GL) theory [18] that, although not sensitive to microscopic details, is accurate and simple enough to describe the fluctuations above T_c. While the transport experiments like the Nernst effect have some hotly debated experimental [19] and theoretical [20–23] issues to be addressed, the clearest data come from recent thermodynamical measurements of magnetization [24] in LSCO, $Bi_2Sr_2CaCu_2O_{8+\delta}$ (BSCCO), and $YBa_2Cu_3O_7$ (YBCO) [17].

The purpose of this paper is to provide a convincing theoretical description of the magnetization data. Our conclusion is that the GL description of the layered materials LSCO, BSCCO, and YBCO by the Lawrence-Doniach model within the self-consistent fluctuation theory (SCFT, sometimes referred to as Hartree approximation) fits well the fluctuation effects in major families of HTSC materials in wide range of fields and temperatures and demonstrates that the fluctuation effects extend to well above T_c. This means that there is no evidence that the pseudogap physics directly influences the diamagnetism.

Strong diamagnetism of a type II superconductor takes a form of a network of Abrikosov flux lines (vortices) created by magnetic field. Vortices strongly interact with each other creating highly correlated configurations. A generic magnetic phase diagram of HTSC [25,26], Fig. 1, contains four phases: two inhomogeneous phases, unpinned crystal and pinned Bragg glass, and two homogeneous phases, unpinned vortex liquid and pinned vortex glass. In HTSC thermal fluctuations are strong enough to melt the lattices [27] into the vortex liquid over a very large portion of the phase diagram. The glass line separates pinned vortex matter (zero resistivity) from the unpinned one (nonzero resistivity due to flux flow). The vortex liquid portion covers the fields (up to $40T$) and temperatures (above and below T_c) of the magnetization experiments [17].

Fluctuation diamagnetism in type II superconductors has been studied theoretically [18] within both the microscopic theory (starting from the pioneering work of Aslamazov and Larkin) and the GL approach. In all of these calculations (with

*lidp@pku.edu.cn
†vortexbar@yahoo.com

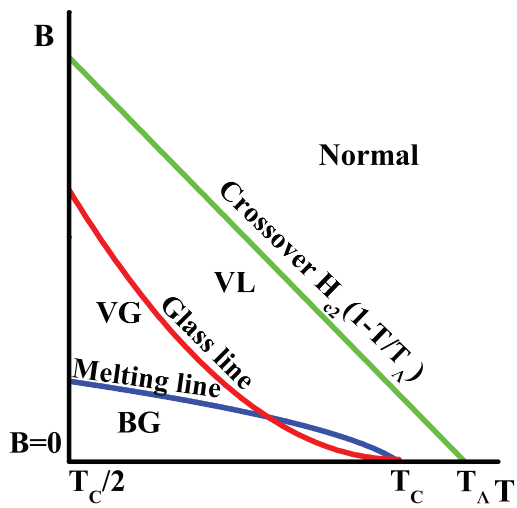

FIG. 1. (Color online) Magnetic phase diagram of high-T_c superconductors. VL is the vortex liquid region, while VG and BG are the vortex glass and Bragg glass, respectively.

an exception of the strong field limit that allows the lowest Landau level approximation, see Ref. [28]) the fluctuations were assumed to be small enough, so they can be taken into account perturbatively. Within the GL approach the leading order in fluctuations was termed the Gaussian fluctuation theory (GFT) [18,29–33]. The GFT applied to the recent HTSC magnetization data was criticized [34,35] to fit just a single curve (magnetic field) rather than a significant portion of the magnetic phase diagram near T_c. To determine theoretically fluctuation diamagnetism for strong thermal fluctuations, one therefore must go beyond this simple approximation neglecting the effect of the quartic term in the GL free energy. The effect of the quartic term is taken into account within SCFT, widely used in physics of phase transitions at zero magnetic field, and was adapted to transport property in magnetic field [36,37]. Since disorder is not considered, our results are limited to the vortex liquid phase of the magnetic phase diagram of Fig. 1, where vortices are depinned.

The paper is organized as follows. In Sec. II, the Lawrence-Doniach GL model of layered superconductors is briefly introduced. We then, in Sec. III, set up the general formalism of the SCFT method, and particularly calculate the magnetization of a strongly type II superconductor under a constant and homogeneous magnetic field, by the SCFT under the Lawrence-Doniach GL framework. The SCFT magnetization result is compared with the recent experiments [17] of several typical HTSCs and the GFT method in Sec. IV. We conclude in Sec. V that the diamagnetism in HTSCs above T_c is mainly due to superconducting fluctuations and can be well accounted by the SCFT method.

II. GL MODEL OF LAYERED SUPERCONDUCTOR

The layered superconductor is sufficiently accurately described on the mesoscopic scale by the Lawrence-Doniach free energy (incorporating microscopic thermal fluctuation via dependence of parameters on temperature T, but not containing thermal fluctuations of the order parameter on the mesoscopic scale):

$$F[\psi] = s' \sum_l \int_{\mathbf{r}} \left[\frac{\hbar^2}{2m_a} |\mathbf{D}\psi_l|^2 + \frac{\hbar^2}{2m_c d'^2} |\psi_l - \psi_{l+1}|^2 + \alpha(T - T_\Lambda)|\psi_l|^2 + \frac{\beta}{2}|\psi_l|^4 \right]. \quad (1)$$

Here $\psi_l(x,y)$ is the order parameter in the l^{th} layer, $\mathbf{D} \equiv \nabla + \frac{ie^*}{\hbar c}\mathbf{A}$, is the covariant derivative ($e^* = 2|e|$) and $\mathbf{A}$ is the vector potential of magnetic field oriented along the crystallographic c axis. The (effective) layer thickness is s' and the distance between the layers is d'. Note that the temperature T_Λ, which will be called mean field or bare transition temperature, is larger than the real transition temperature T_c.

The bare coherence length $\xi = \hbar/\sqrt{2m_a\alpha T_\Lambda}$ will be used as the unit of length and the upper critical field $H_{c2} \equiv \hbar c/e^*\xi^2$ as the magnetic field unit. They depend on the coarse graining scale (cutoff scale Λ) at which the mesoscopic model is derived (in principle). The dimensionless order parameter is $\phi = \sqrt{\beta/2\alpha T_\Lambda}\psi$, so that the GL Boltzmann factor in scaled units takes a form,

$$f = \frac{F}{T} = \frac{1}{2\omega_\Lambda t_\Lambda} \sum_l \int_{\mathbf{r}} [|\mathbf{D}\phi_l|^2 + d^{-2}|\phi_l - \phi_{l+1}|^2 - (1 - t_\Lambda)|\phi_l|^2 + |\phi_l|^4]. \quad (2)$$

Here $t_\Lambda = T/T_\Lambda$, $b = B/H_{c2}$ are the dimensionless temperature and induction. It is more convenient to use the fluctuation strength parameter $\omega_\Lambda = \sqrt{2Gi_\Lambda}\pi/s$, instead of the more customary (bare) Ginzburg number $\mathrm{Gi}_\Lambda = 2(e^*/c\hbar)^3 \kappa^4 T_\Lambda^2 \gamma^2/H_{c2}$. Since the renormalization by strong thermal fluctuations is central in this work, bare quantities carry index Λ, although the results used for fitting experiments will utilize renormalized parameters. The anisotropy $\gamma = \sqrt{m_c/m_a}$, $s = s'\gamma/\xi_\Lambda$, and $d = d'\gamma/\xi_\Lambda$. In strongly type II superconductors the Ginzburg parameter $\kappa = \lambda/\xi \gg 1$ and magnetic field is nearly homogeneous, so we choose the Landau gauge $\mathbf{A} = (-by, 0)$ in $\mathbf{D} = \nabla + i\mathbf{A}$.

III. FLUCTUATION DIAMAGNETISM CALCULATED WITHIN SCFT

A. Self-consistent approximation

The self-consistent approximation theory (SCFT, also sometimes called the variational Gaussian approximation theory) can be presented in many different ways. Here we use a variational (minimal sensitivity principle [38]) derivation along the lines of the more general optimized expansion [39]. Here we apply it to calculate the fluctuation magnetization of the type II superconductor described within the GL approach by free energy, Eq. (1).

Generally, the partition function is the functional integral over the Boltzmann factor,

$$Z = \int \mathcal{D}\psi\mathcal{D}\psi^* \exp(-f[\psi]). \quad (3)$$

The idea of the method [28] is as follows: Let us divide the Boltzmann factor $f[\phi]$ into an optimized quadratic (large) part, $K[\psi,\varepsilon]$ and a small perturbation $W[\psi,\varepsilon]$, where ε is the variational parameter, the vortex liquid gap in our case, which is found from minimization of the variational free energy including the fluctuations on the mesoscopic scale.

Then the free energy is expanded to first order in W:

$$F(\varepsilon) = -T\ln Z = -T\ln\int_\psi \exp[-(K+W)]$$
$$= -T\ln\int_\psi e^{-K}(1-W) = -T\ln Z_0 + T\langle W\rangle_0. \quad (4)$$

Here unperturbed quantities Z_0 and $\langle W\rangle_0$ are defined as

$$Z_0 = \int_\psi e^{-K}, \quad \langle W\rangle_0 = Z_0^{-1}\int_\psi W e^{-K}. \quad (5)$$

The gap equation, determining ε variationally, is

$$\frac{d}{d\varepsilon}F(\varepsilon) = 0. \quad (6)$$

The method is very general, but the presence of magnetic field and UV cutoff makes its application nontrivial.

B. Magnetization of the Lawrence-Doniach GL model in strongly type II superconductors

Gibbs energy of Lawrence Doniach model is

$$G[\psi,A] = s'\sum_l\int_{\mathbf{r}}\left[F[\psi,A] + \frac{(B_l-H)^2}{8\pi}\right]. \quad (7)$$

For constant homogeneous external magnetic field, we shall calculate the partition function of the Gibbs ensemble,

$$Z = \int \mathcal{D}\mathbf{A}\mathcal{D}\psi\mathcal{D}\psi^* e^{-G[\psi,A]/T}. \quad (8)$$

Performing the same rescaling of fields as in Sec. II, the Boltzmann weight becomes: $g \equiv G/T = f[\phi,b] + f_{\text{mag}}[b]$, where f is given in Eq. (2) and

$$f_{\text{mag}}[b] = \frac{\kappa^2}{4\omega_\Lambda t_\Lambda}\sum_l\int_{\mathbf{r}}(b_l-h)^2. \quad (9)$$

Therefore thermodynamic (effective) Gibbs energy density,

$$\mathcal{G} = -d\omega_\Lambda t_\Lambda V^{-1}\ln Z, \quad (10)$$

defined as dimensionless thermodynamic Gibbs energy, which determines the magnetization inside superconducting layer $\langle b_l - h\rangle/(4\pi)$ via

$$\frac{b_l-h}{4\pi} = -\frac{1}{2\pi\kappa^2}\frac{\partial(\mathcal{G}(h))}{\partial h}$$
$$= -\frac{d}{4\pi V}Z^{-1}\int_{\mathbf{A},\psi}\sum_l\int_{\mathbf{r}}(b_l-h)\,e^{-G[\psi,A]/T}. \quad (11)$$

Since $\kappa \gg 1$ magnetization is small $\langle b_l-h\rangle/(4\pi) \sim \kappa^{-2}h$, and it suffices to consider a simpler statistical sum

$$Z \approx \int_\phi e^{-f[\phi,h]}. \quad (12)$$

Thermodynamic Gibbs energy density $\mathcal{G}(h)$ in $\frac{\partial(\mathcal{G}(h))}{\partial h}$ of Eq. (11) can be approximated as $-d\omega_\Lambda t_\Lambda V^{-1}\ln Z$ where Z is given in Eq. (12). Next we will use the self-consistent approximation to calculate $\ln Z$.

C. Application of the self-consistent method in the presence of magnetic field

The only nontrivial technical difficulty is the summation over Landau levels in the presence of UV cutoff Λ.

We take $f[\phi,b] = K + W$, which are defined below,

$$K = \frac{1}{2\omega_\Lambda t_\Lambda}\sum_l\int_{\mathbf{r}}[|\mathbf{D}\phi_l|^2 + d^{-2}|\phi_l - \phi_{l+1}|^2$$
$$+(2\varepsilon - b)|\phi_l|^2], \quad (13)$$

$$W = \frac{1}{2\omega_\Lambda t_\Lambda}\sum_l\int_{\mathbf{r}}[(t_\Lambda + b - 1 - 2\varepsilon)|\phi_l|^2 + |\phi_l|^4]. \quad (14)$$

The zero-order partition function Z_0 is the form of Gaussian functional integral. The order parameter $\phi_l(r)$ is expanded in eigenfunctions [28],

$$\phi_l(r) = \frac{1}{(2\pi)^{3/2}}\sum_n\int_{\mathbf{q}}\int_{k=0}^{2\pi/d} e^{ildk}\varphi_{n,\mathbf{q}}\phi_{k,\mathbf{q},n}, \quad (15)$$

where k is the wave vector in c direction and $\varphi_{n,\mathbf{q}}$ is the Landau's quasimomentum wave function that obeys

$$-\frac{1}{2}\mathbf{D}^2\varphi_{n,\mathbf{q}} = \left(n+\frac{1}{2}\right)b\varphi_{n,\mathbf{q}}. \quad (16)$$

The $\mathbf{q}$ integration is over the Abrikosov lattice Brillouin zone (applicable even when the lattice melts [28]) with area $2\pi b$. In this basis

$$Z_0 = \int_\psi \exp\left\{-\frac{1}{\omega_\Lambda t_\Lambda d}\sum_{n=0}^{\infty}\int_{\mathbf{q}}\int_{k=0}^{2\pi/d}\right.$$
$$\left.\times\left[\frac{1}{d^2}(1-\cos(kd)) + nb + \varepsilon\right]\phi_{k,\mathbf{q},n}\phi^*_{k,\mathbf{q},n}\right\}. \quad (17)$$

The Gaussian integral results in

$$\ln Z_0 = -\frac{Vb}{(2\pi)^2}\int_{k=0}^{2\pi/d}\sum_{n=0}^{N_{\max}(\Lambda)}\ln[gb+nb], \quad (18)$$

$$g \equiv (1-\cos(kd))/(d^2b) + \varepsilon/b. \quad (19)$$

It is not *a priori* clear how to trade the energy cutoff Λ to maximal Landau level. However the physical requirement of renormalizability of the SCFT, namely that a physical quantity should be cutoff independent near criticality. This unambiguously leads to

$$(N_f+1)b = \Lambda. \quad (20)$$

With this upper limit the sum can be done

$$\mathcal{G}_0 = -V^{-1}d\omega_\Lambda t_\Lambda \ln Z_0$$
$$= \frac{d\omega_\Lambda t_\Lambda b}{(2\pi)^2}\int_{k=0}^{2\pi/d}\left[\frac{\Lambda}{b}\ln b + \ln\frac{\Gamma(g+\Lambda/b)}{\Gamma(g)}\right], \quad (21)$$

where g is given in Eq. (19).

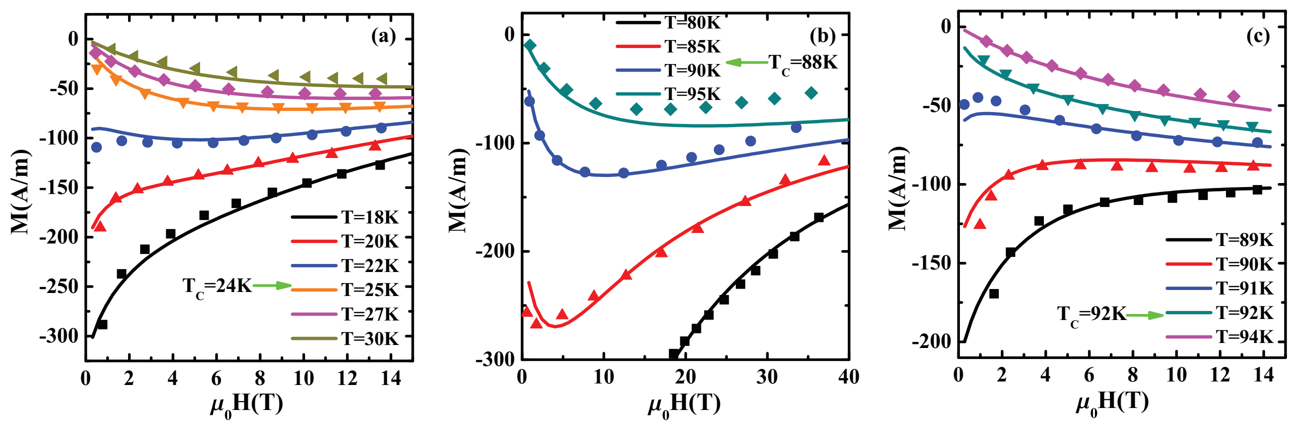

FIG. 2. (Color online) Magnetization data of Ref. [17] (dots) and their self-consistent approximation fits (solid lines). Three major families of high-T_c superconductors are represented: (a) underdoped LSCO, (b) optimally doped BSCCO, (c) optimally doped YBCO. The curve closest to T_c for each sample were used to determine the fitting parameters given in Table I. Each set of curves uses just three fitting parameters.

It is convenient to express the average of the superfluid density via derivative with respect to variational parameter:

$$\langle|\phi_l|^2\rangle_0 = Z_0^{-1}\int_\phi |\phi_l|^2 e^{-K} = \frac{\partial \mathcal{G}_0}{\partial \varepsilon} = \frac{d\omega_\Lambda t_\Lambda}{(2\pi)^2}\int_{k=0}^{2\pi/d}[\psi(g+\Lambda/b)-\psi(g)]. \tag{22}$$

Combining Eqs. (4), (21), and (22) we finally arrive at the Gibbs energy density of the system,

$$\mathcal{G} = \mathcal{G}_0 - \left(\varepsilon + \frac{1-t_\Lambda - b}{2}\right)\frac{\partial \mathcal{G}_0}{\partial \varepsilon} + \left(\frac{\partial \mathcal{G}_0}{\partial \varepsilon}\right)^2. \tag{23}$$

Following Eq. (6), the vortex liquid gap equation is arrived by minimizing the Gibbs energy density of the system $\partial\mathcal{G}/\partial\varepsilon = 0$.

$$\varepsilon = \frac{t_\Lambda + b - 1}{2} + \frac{\omega_\Lambda t_\Lambda d}{2\pi^2}\int_{k=0}^{2\pi/d}\left[\psi\left(g+\frac{\Lambda}{b}\right) - \psi\left(g\right)\right]; \tag{24}$$

where ψ is the $\digamma$ function (digamma function). The integration is over the Fourier harmonics k in the c direction.

The SCFT is widely used in GL model without magnetic field, $b = 0$, under the name of mean field and in this case simplifies to

$$\begin{aligned}\varepsilon &= (t_\Lambda - 1)/2 + \omega_\Lambda t_\Lambda[h(\Lambda+\varepsilon) - h(\varepsilon)];\\ h(x) &= \ln\left(1 + xd^2 + \sqrt{2xd^2 + (xd^2)^2}\right)/\pi.\end{aligned} \tag{25}$$

In this case ε has a meaning of the mass of the field ϕ describing the fluctuations in the normal phase. It vanishes at the renormalized transition temperature T_c leading to its relation to T_Λ

$$T_\Lambda^{-1} = T_c^{-1}[1 - 2\omega h(\Lambda)]. \tag{26}$$

Here the renormalized coupling $\omega = \sqrt{2Gi}\pi/s$, this time expressed via renormalized Ginzburg number $\mathrm{Gi} = 2\left(e^*/c\hbar\right)^3 \kappa^4 T_c^2 \gamma^2/H_{c2}$, is used. Expressing T_Λ via T_c in Eq. (24), the gap equation becomes,

$$\begin{aligned}\varepsilon = {} & \frac{\omega t d}{2\pi^2}\int_{k=0}^{2\pi/d}[\psi(g+\Lambda/b) - \psi(g)]\\ & - \omega t h(\Lambda) + (t + b - 1)/2,\end{aligned} \tag{27}$$

with $t = T/T_c$. Physical quantities are then calculated using numerical solution of this algebraic equation. For $b,\varepsilon \ll \Lambda$ it is cutoff independent and simplifies:

$$\varepsilon = (t + b - 1)/2 - \frac{\omega t d}{2\pi^2}\int_{k=0}^{2\pi/d}[\psi(g) + \ln 2]. \tag{28}$$

The magnetization is $\langle b_l - h\rangle/(4\pi)$ inside the superconducting layer, therefore the average magnetization in the whole sample is $(s/d)\langle b_l - h\rangle/(4\pi)$. $\langle b_l - h\rangle/(4\pi)$ can be obtained by Eq. (11) and Eq. (23). The average magnetization in the sample results in

$$\begin{aligned}M = {} & \frac{\omega s t H_{c2}}{8\pi^3\kappa^2}\int_{k=0}^{2\pi/d}\{(g + \Lambda/b - 1/2)\psi(g+\Lambda/b)\\ & - (g - 1/2)\psi(g) + \ln[\Gamma(g)/\Gamma(g+\Lambda/b)] - \Lambda/b\},\end{aligned} \tag{29}$$

while for $b,\varepsilon \ll \Lambda$ it simplifies to

$$M = \frac{\omega s t H_{c2}}{8\pi^3\kappa^2}\int_{k=0}^{2\pi/d}\left[\ln\frac{\Gamma(g)}{\sqrt{2\pi}} + g - \left(g - \frac{1}{2}\right)\psi(g)\right]. \tag{30}$$

In certain portions of the magnetic phase diagrams the strong inequalities $b,\varepsilon \ll \Lambda$ are not obeyed, while SCFT is still valid, so we have used the formula Eq. (29), with weak (logarithmic) cutoff dependence instead of the cutof-independent renormalized formula.

IV. COMPARING WITH EXPERIMENTS AND GFT

Recent accurate magnetization data [17] on magnetization of three major families of HTSC materials, including underdoped $La_{2-x}Sr_xCuO_4$ for $x = 0.09$, optimally doped $Bi_2Sr_2CaCu_2O_{8+\delta}$, and optimally doped $YBa_2Cu_3O_7$, are fitted in Figs. 2(a)–2(c), respectively. Measured magnetization

TABLE I. Fitting parameters for LSCO, BSCCO, and YBCO.

Material	T_c (Kelvin)	d' (Angstrom)	H_{c2} (Tesla)	T_Λ (Kelvin)	γ	Λ	κ	Gi
LSCO	24	6.58	31	33	29	0.30	66.7	0.033
BSCCO	88	19.6	115	99	19	0.25	55.6	0.025
YBCO	92	11.68	220	100	4.1	0.22	78.7	0.0026

curves of LSCO and YBCO in the 0–14T field range and BSCCO at 0–40T show distinct features above and below T_c, thus allowing meaningful fitting. The theoretical magnetization just below T_c is nonmonotonic, consistent with the experiment, see Fig. 2(c). The conditions $b,\varepsilon \ll \Lambda$ are obeyed provided temperature does not deviate too far from T_c and magnetic field is small compared to H_{c2}. Several temperatures within 10% of T_c were used to determine three fitting parameters, H_{c2}, anisotropy γ, and κ^2/s, using simplified formulas Eqs. (28), (30). The interlayer distances d' were taken from Ref. [40]. Near T_c, the correlation length is large, therefore we take $s = d$, as the maximum value of s. The results for each material are given in Table I. For the rest of the data (higher temperature and higher magnetic field) the theoretical curves shown in Fig. 2 were logarithmically dependent on cutoff and therefore the full formulas, Eqs. (24), (29), were utilized. The two additional parameters, namely mean field critical temperature T_Λ and Λ are constrained via Eq. (26) (with experimentally measured T_c also listed in Table I). The values of T_Λ and Λ in units of $\hbar e^* H_{c2}/(m_a c)$ are given in Table I.

To demonstrate the importance of nonperturbative effects, the SCFT magnetization Eq. (29) is compared with GFT within the two-dimensional (2D) layered superconductors model [30] in Fig. 3. One observes that the SCFT magnitude is much smaller than the GFT one. One of the reasons is that the vortex liquid gap ε is larger than the reduced temperature (perturbative gap) $(t_\Lambda + b - 1)/2$. The data of Ref. [17] in the region of smaller fields exhibit the so-called intersection point of the magnetization curves plotted as function of temperature. Our magnetization curves (underdoped LSCO is shown in Fig. 4 as an example) demonstrate the intersection point in this region for all three materials. The intersection points, defined as

$$\frac{\partial M(T,B)}{\partial T}|_{T=T_{cr}(B)} = 0, \tag{31}$$

were measured in many high-T_c cuprate [41–43] and explained within the lowest Landau level approximation [45,46] valid for $\varepsilon \ll b$. It turns out that an addition requirement for the intersection point is $\varepsilon d^2 \gg 1$.

There has been a debate on whether in underdoped HTSC there is a second, high field intersection point above T_c in underdoped materials, in particular [44] in underdoped LSCO for $x = 0.81$ and 0.071. We find no such point in our calculations as shown in Fig. 5(c) and Fig. 5(d) for both underdoped LSCO with $x = 0.09$ ($La_{2-x}Sr_xCuO_4$ [17]) and strongly underdoped BSCCO with $T_c = 50\,K$ ($La_{2-x}Sr_xCuO_4$ [12]). From Figs. 5(b), 5(d), there are good interaction points for underdoped BSCCO from 1T to 4T, and for LSCO09 from 1T to 6T. Figures 5(c), 5(d) are plotted by the SCFT using fitting parameters in Table I (they shall be essentially the same as the experimental plot due to the high accurate fitting in Fig. 2). The data of $La_{2-x}Sr_xCuO_4$ [44] in the strongly underdoped LSCO samples at very large magnetic field above T_c therefore cannot be fitted by our theory. Noting that in this region of the second intersection point of $La_{2-x}Sr_xCuO_4$ [44], the diamagnetic signal is smaller than background by order of magnitude, therefore the existence of the second intersection point is not convincing.

V. CONCLUSIONS

We have investigated the fluctuation diamagnetism of HTSC using a self consistent nonperturbative method beyond

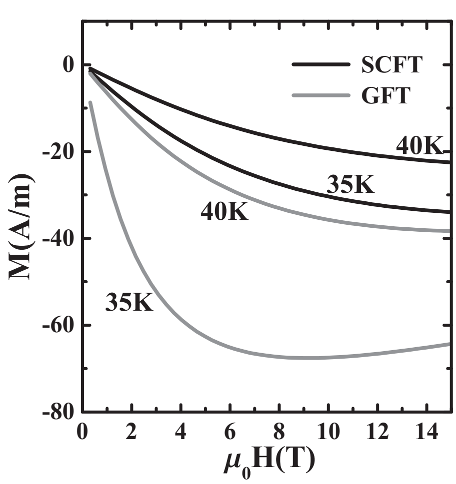

FIG. 3. The comparison between the fluctuation magnetization of LSCO calculated using the self-consistent fluctuation theory (SCFT) vs the perturbative gaussian fluctuation (GFT) one.

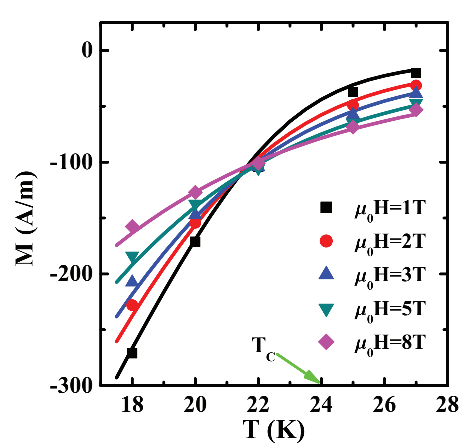

FIG. 4. (Color online) Fit of magnetization [17] in the region of the intersection point [fields lower than those shown in Fig. 2(a)] in LSCO using the same fitting parameters (given in Table I).

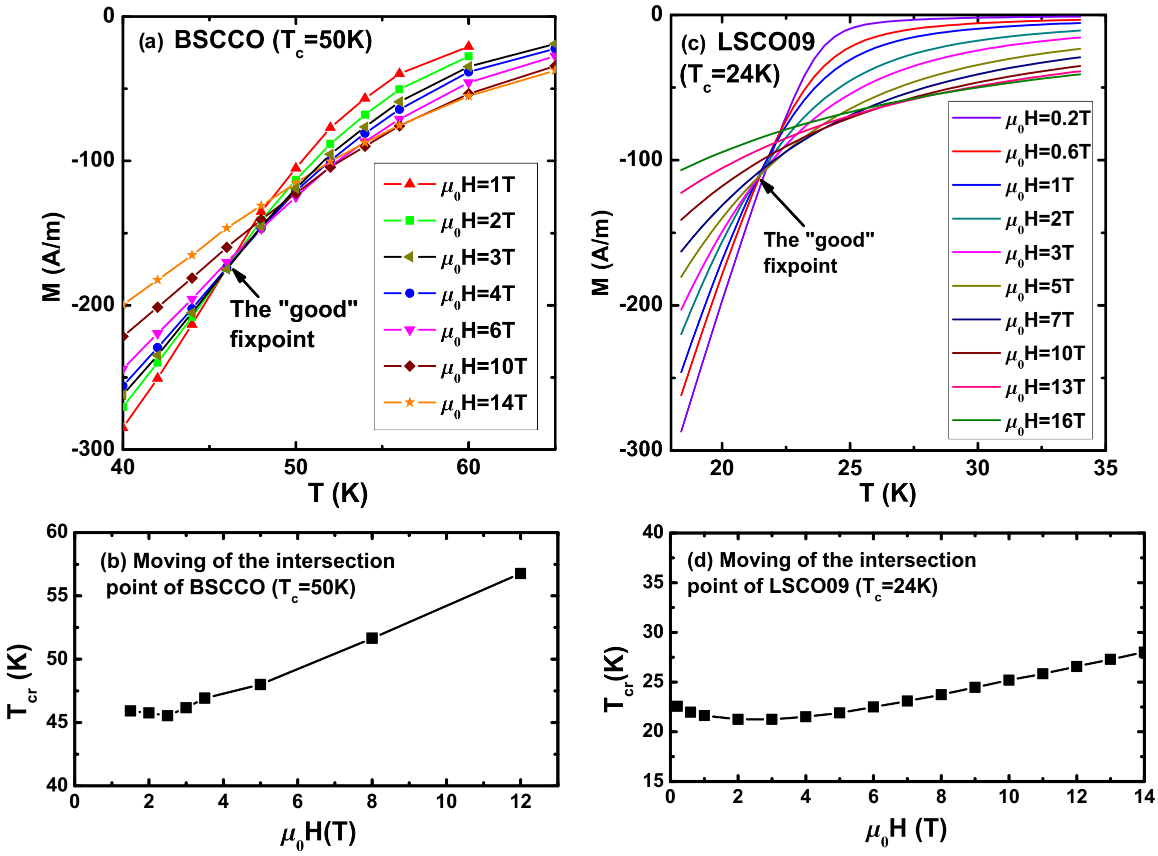

FIG. 5. (Color online) (a) Magnetization data of underdoped BSCCO (Bi 2212, $T_c = 50\,\mathrm{K}$) in Ref. [12] (dots) and (b) their intersection point. (c) Magnetization of slightly underdoped LSCO09 ($T_c = 24\,\mathrm{K}$) calculated by the self-consistent fluctuation theory (SCFT), using the fitting parameters in Table I and (d) their intersection point.

Gaussian fluctuations term within Lawrence-Doniach GL model. The comparison with recent accurate experiments near T_c demonstrate that the effect of quartic terms should to be included due to strong fluctuations. The theory describes well a wide class of materials from relatively low anisotropy optimally doped YBCO to highly anisotropic underdoped LSCO and optimally doped BSCCO at temperatures both below and above T_c. No input from the microscopic pseudogap physics is needed to describe the diamagnetism data. Dynamical effects like the Nernst effect, electrical, and thermal conductivity can be in principle approached within the similar SCFT generalized to time-dependent variants of the GL model. The method used in the present paper can also apply to strong type II low-T_c superconductors. The diamagnetization due to the superconducting fluctuation was also observed in MgB_2, a low-T_c superconductor [47].

At last we address the ongoing recent controversy [33–35] regarding the location of the $H_2(T)$ crossover and the nonmonotonic behavior of magnetization below T_c. In $La_{2-x}Sr_xCuO_4$ [35] it was pointed out that the result of the GFT result for optimally doped YBCO is similar to that of low-T_c materials with negligible renormalization of T_c (see Fig. 3(a) in $La_{2-x}Sr_xCuO_4$ [35]). Our phase diagram, Fig. 1, is consistent with their Fig. 3(b) based on the experiment. Moreover our magnetization just below T_c is in fact nonmonotonic, see Fig. 2(c), consistent with the experiment. Our calculation supports the phase-disordering picture of fluctuations advocated by $La_{2-x}Sr_xCuO_4$ [35], thus the present work resolves the controversy by using the SCFT calculation of the Lawrence-Doniach GL model. However, various experiments also show that there are other types of ordered states inside the pseudogap phase [5]. It remains an important open problem to sort out the different types of order and order parameter fluctuations [24].

ACKNOWLEDGMENTS

The work of D.L. and X.J. is supported by the National Natural Science Foundation of China (Grant No. 11274018), B.R. is supported by NSC of the Republic of China (Grant No. 8907384-98N097) and AOE program.

[1] T. Timusk and B. Statt, Rep. Prog. Phys. 62, 61 (1999).
[2] M. N. Norman, D. Pines, and C. Kallin, Adv. Phys. 54, 715 (2005).
[3] P. A. Lee, N. Nagaosa, and X.-G. Wen, Rev. Mod. Phys. 78, 17 (2006).
[4] K. Hur and T. M. Rice, Ann. Phys. (N.Y.) 324, 1452 (2009).

[5] D. Scalapino, Rev. Mod. Phys. **84**, 1383 (2012).
[6] V. J. Emery and S. A. Kivelson, Nature (London) **374**, 434 (1995).
[7] P. A. Lee and X. G. Wen, Phys. Rev. Lett. **78**, 4111 (1997).
[8] A. Levchenko, M. R. Norman, and A. A. Varlamov, Phys. Rev. B **83**, 020506 (2011).
[9] Z. A. Xu, N. P. Ong, Y. Wang, T. Kakeshita, and S. Uchida, Nature (London) **406**, 486 (2000).
[10] Y. Wang, Z. A. Xu, T. Kakeshita, S. Uchida, S. Ono, Y. Ando, and N. P. Ong, Phys. Rev. B **64**, 224519 (2001).
[11] Y. Wang, N. P. Ong, Z. A. Xu, T. Kakeshita, S. Uchida, D. A. Bonn, R. Liang, and W. N. Hardy, Phys. Rev. Lett. **88**, 257003 (2002).
[12] Y. Wang, Lu Li, and N. P. Ong, Phys. Rev. B **73**, 024510 (2006).
[13] F. Rullier-Albenque, H. Alloul, and G. Rikken, Phys. Rev. B **84**, 014522 (2011), and references therein.
[14] M. S. Grbic, M. Pozek, D. Paar, V. Hinkov, M. Raichle, D. Haug, B. Keimer, N. Barisic, and A. Dulcic, Phys. Rev. B **83**, 144508 (2011).
[15] Y. J. Chen, P. J. Lin, K. H. Wu, B. Rosenstein, C. W. Luo, J. Y. Juang, and J. Y. Lin, Supercond. Sci. Technol. **26**, 105029 (2013).
[16] K. Kudo, M. Yamazaki, T. Kawamata, T. Adachi, T. Noji, Y. Koike, T. Nishizaki, and N. Kobayashi, Phys. Rev. B **70**, 014503 (2004).
[17] Lu Li, Y. Wang, S. Komiya, S. Ono, Y. Ando, G. D. Gu, and N. P. Ong, Phys. Rev. B **81**, 054510 (2010); Y. Wang, Lu Li, M. J. Naughton, G. D. Gu, S. Uchida, and N. P. Ong, Phys. Rev. Lett. **95**, 247002 (2005).
[18] A. Larkin and A. Varlamov, *Theory of Fluctuations in Superconductors* (Clarendon Press, Oxford, 2005).
[19] J. Chang, N. Doiron-Leyraud, O. Cyr-Choinire, G. Grissonnanche, F. Lalibert, E. Hassinger, J-Ph. Reid, R. Daou, S. Pyon, T. Takayama, H. Takagi, and Louis Taillefer, Nature Phys. **8**, 751 (2012).
[20] I. Ussishkin, S. L. Sondhi, and D. A. Huse, Phys. Rev. Lett. **89**, 287001 (2002).
[21] A. Sergeev, M. Y. Reizer, and V. Mitin, Phys. Rev. B **77**, 064501 (2008); Phys. Rev. Lett. **106**, 139701 (2011).
[22] M. N. Serbyn, M. A. Skvortsov, A. A. Varlamov, and V. Galitski, Phys. Rev. Lett. **102**, 067001 (2009); **106**, 139702 (2011).
[23] K. Michaeli and A. M. Finkel'stein, Phys. Rev. B **80**, 115111 (2009); **80**, 214516 (2009).
[24] S. A. Kivelson and E. H. Fradkin, Physics **3**, 15 (2010).
[25] D. Li and B. Rosenstein, Phys. Rev. Lett. **90**, 167004 (2003); Phys. Rev. B **70**, 144521 (2004).
[26] H. Beidenkopf, T. Verdene, Y. Myasoedov, H. Shtrikman, E. Zeldov, B. Rosenstein, D. Li, and T. Tamegai, Phys. Rev. Lett. **98**, 167004 (2007).
[27] E. Zeldov, D. Majer, M. Konczykowski, V. B. Geshkenbein, V. M. Vinokur, and H. Shtrikman, Nature (London) **375**, 373 (1995).
[28] B. Rosenstein and D. Li, Rev. Mod. Phys. **82**, 109 (2010).
[29] R. E. Prange, Phys. Rev. B **1**, 2349 (1970).
[30] C. Carballeira, J. Mosqueira, A. Revcolevschi, and F. Vidal, Phys. Rev. Lett. **84**, 3157 (2000); Physica C **384**, 185 (2003).
[31] P. Carretta, A. Lascialfari, A. Rigamonti, A. Rosso, and A. Varlamov, Phys. Rev. B **61**, 12420 (2000).
[32] A. Lascialfari, A. Rigamonti, L. Romano, A. A. Varlamov, and I. Zucca, Phys. Rev. B **68**, 100505 (2003).
[33] R. I. Rey, A. Ramos-Alvarez, J. Mosqueira, M. V. Ramallo, and F. Vidal, Phys. Rev. B **87**, 056501 (2013).
[34] L. Cabo, J. Mosqueira, and F. Vidal, Phys. Rev. Lett. **98**, 119701 (2007); N. P. Ong, Y. Wang, Lu Li, and M. J. Naughton, *ibid.* **98**, 119702 (2007).
[35] Lu Li, Y. Wang, and N. P. Ong, Phys. Rev. B **87**, 056502 (2013).
[36] S. Ullah and A. T. Dorsey, Phys. Rev. B **44**, 262 (1991); Phys. Rev. Lett. **65**, 2066 (1990).
[37] B. D. Tinh and B. Rosenstein, Phys. Rev. B **79**, 024518 (2009); B. D. Tinh, D. Li, and B. Rosenstein, *ibid.* **81**, 224521 (2010).
[38] P. M. Stevenson, Phys. Rev. D **30**, 1712 (1984); A. Kovner and B. Rosenstein, *ibid.* **39**, 2332 (1989).
[39] D. Li and B. Rosenstein, Phys. Rev. B **65**, 024513 (2001); H. Kleinert, *Path Integrals in Quantum Mechanics, Statistics, Polymer Physics, and Financial Markets* (World Scientific, Singapore, 2009).
[40] C. P. Poole, Jr., H. A. Farach, R. J. Creswick, and R. Prozorov, *Superconductivity* (Academic Press, Amsterdam, 2007).
[41] S. Salem-Sugui, Jr., J. Mosqueira, and A. D. Alvarenga, Phys. Rev. B **80**, 094520 (2009); S. Salem-Sugui, Jr., A. D. Alvarenga, J. Mosqueira, J. D. Dancausa, C. Salazar Mejia, E. Sinnecker, H. Luo, and H. Wen, Supercond. Sci. Technol. **25**, 105004 (2012); J. Mosqueira, L. Cabo, and F. Vidal, Phys. Rev. B **76**, 064521 (2007).
[42] B. Rosenstein, B. Ya. Shapiro, R. Prozorov, A. Shaulov, and Y. Yeshurun, Phys. Rev. B **63**, 134501 (2001).
[43] M. J. Naughton, Phys. Rev. B **61**, 1605 (2000).
[44] Y. M. Huh and D. K. Finnemore, Phys. Rev. B **65**, 092506 (2002).
[45] Z. Tesanovic, L. Xing, L. Bulaevskii, Q. Li, and M. Suenaga, Phys. Rev. Lett. **69**, 3563 (1992).
[46] Fareh Pei-Jen Lin and B. Rosenstein, Phys. Rev. B **71**, 172504 (2005).
[47] A. Lascialfari, T. Mishonov, A. Rigamonti, P. Tedesco, and A. Varlamov, Phys. Rev. B **65**, 180501 (2002).